



# The Association between the Magnetic Resonance Imaging Findings of Adhesive Capsulitis and Shoulder Muscle Fat Quantification Using a Multi-Echo Dixon Method

Min A Yoon, MD<sup>1</sup>, Suk-Joo Hong, MD<sup>1</sup>, Sun Hong, MD<sup>1</sup>, Chang Ho Kang, MD<sup>2</sup>, Baek Hyun Kim, MD<sup>3</sup>, In Seong Kim, PhD<sup>4</sup>

<sup>1</sup>Department of Radiology, Korea University Guro Hospital, Korea University College of Medicine, Seoul 08308, Korea; <sup>2</sup>Department of Radiology, Korea University Anam Hospital, Korea University College of Medicine, Seoul 02841, Korea; <sup>3</sup>Department of Radiology, Korea University Ansan Hospital, Korea University College of Medicine, Ansan 15355, Korea; <sup>4</sup>Siemens Healthcare, Seoul 03737, Korea

**Objective:** To investigate the association between the magnetic resonance imaging (MRI) findings of adhesive capsulitis and shoulder muscle fat percentages using a multi-echo Dixon method.

**Materials and Methods:** Twenty-four patients with clinical diagnoses of adhesive capsulitis and either intact rotator cuffs or Ellman grade 1 partial tears as indicated by MRI scans were included. Two radiologists independently evaluated MRI scans of adhesive capsulitis as follows: presence or absence of axillary recess capsular and extracapsular hyperintensities; thickness of the coracohumeral ligament; thickness of abnormal rotator interval soft tissue; and thickness of glenoidal/humeral axillary recess capsules. Fat quantifications of the supraspinatus, infraspinatus, teres minor, subscapularis, teres major and posterior deltoid muscles were performed using multi-echo Dixon imaging at three locations. Inter-rater agreement was assessed. Differences in fat percentages were assessed and correlations between fat percentages and quantitative measurements were evaluated.

**Results:** The fat percentage of the supraspinatus was significantly higher in patients with extracapsular hyperintensity (present,  $3.00 \pm 1.74\%$ ; absent,  $1.81 \pm 0.80\%$ ;  $p = 0.022$ ). There were positive correlations between the fat percentage of the teres minor and the thicknesses of the abnormal rotator interval soft tissue ( $r = 0.494$ ,  $p = 0.014$ ) and the glenoidal axillary recess capsule ( $r = 0.475$ ,  $p = 0.019$ ). After controlling for the effects of age, sex and clinical stage, the relationship between the teres minor fat percentage and the thickness of the abnormal rotator interval soft tissue was statistically significant ( $r = 0.384$ ,  $p = 0.048$ ). Inter-rater agreement was almost perfect for fat quantification (intraclass correlation coefficients [ICC] > 0.9) and qualitative analyses ( $k = 0.824$ ), but were variable for quantitative measurements (ICC, 0.170–0.606).

**Conclusion:** Several MRI findings of adhesive capsulitis were significantly related to higher fat percentages of shoulder muscles.

**Keywords:** Adhesive capsulitis; Fatty quantification; Shoulder; Rotator cuff; MRI

## INTRODUCTION

Adhesive capsulitis is a common disorder of the shoulder. It affects 3–5% of the population; patients with diabetes and thyroid disease experience a higher incidence rate (1). It is characterized by a painful restriction of shoulder motion that results in fibrosis and contracture of the glenohumeral joint capsule (2, 3). The diagnosis and staging of adhesive capsulitis are usually made based on clinical symptoms and physical examination alone (3).

Received February 20, 2017; accepted after revision July 24, 2017.

**Corresponding author:** Suk-Joo Hong, MD, Department of Radiology, Korea University Guro Hospital, Korea University College of Medicine, 148 Gurodong-ro, Guro-gu, Seoul 08308, Korea.

• Tel: (822) 2626-1341 • Fax: (822) 6280-9076

• E-mail: hongsj@korea.ac.kr

This is an Open Access article distributed under the terms of the Creative Commons Attribution Non-Commercial License (<http://creativecommons.org/licenses/by-nc/4.0>) which permits unrestricted non-commercial use, distribution, and reproduction in any medium, provided the original work is properly cited.

However, clinical diagnosis of adhesive capsulitis is often challenging because many conditions in and around the glenohumeral joint manifest with overlapping clinical features, and no diagnostic criteria for adhesive capsulitis has been established yet.

Magnetic resonance imaging (MRI) is a widely used modality in the assessment of shoulder pain. Several characteristics across MRI findings of adhesive capsulitis have been described by prior studies: capsular thickening in the axillary recess; thickening of the coracohumeral ligament (CHL) with the presence of an abnormal soft tissue lesion in the rotator cuff interval; complete obliteration of the fat triangle under the coracoid process; and, hyperintensity of the inferior glenohumeral ligament and extracapsular portion of the axillary recess on T2-weighted fat saturated images (4-7).

A previous study demonstrated that 5-6 weeks of immobilization facilitated a significant decrease in muscle strength and cross-sectional fiber areas (8). Moreover, muscle strength of the external rotators in the shoulders affected by adhesive capsulitis significantly declined (9). Rotator cuff strengthening exercises have shown positive effects on improving the range of motion and functional outcome (10). Because adhesive capsulitis is associated with months to years of shoulder joint pain and immobilization (3), we hypothesized that chronic disuse of the shoulder muscles and changes in muscle strength associated with adhesive capsulitis may be accompanied by fatty infiltration. Specifically, the MRI findings of adhesive capsulitis may be associated with an increase in shoulder muscle fat infiltration. However, to the best of our knowledge, no prior study has investigated the association between the MRI findings of adhesive capsulitis and fat infiltration of the shoulder musculature.

Recently, chemical shift-encoding based water-fat imaging techniques, such as multi-echo Dixon methods, have shown comparable results to single voxel MR spectroscopy in the quantification of fat in skeletal muscles, including rotator cuff muscles (11, 12). So, the purpose of our study was to investigate the association between the MRI adhesive capsulitis findings and the fat percentage of shoulder muscles using a multi-echo Dixon method.

## MATERIALS AND METHODS

### Subjects

This study was approved by our Institutional Review Board

and informed consent was waived (MD 16051). Among the 114 shoulder MRI examinations performed over a five-month period in 2016, 24 patients (10 men, 14 women; mean age, 48.6 years; range, 28-68 years) were enrolled in our study based on the following inclusion criteria: documented clinical suspicion of adhesive capsulitis evaluated by two physicians (i.e., an orthopedic surgeon and a physiatrists, with 21 and 24 years of experience, respectively), including a gradual restriction of motion, capsular pain on palpation, severe nocturnal pain and stiffness; either intact rotator cuff tendons or grade 1 partial tears according to the Ellman classification (i.e., tear depth less than 3 mm of the tendon thickness) (13) same interpretation of MRI scans by two musculoskeletal radiologists; availability of a T2\*-corrected multi-echo Dixon fat quantification map; and the absence of a mass, trauma, prior surgery, infection or inflammatory arthritis in or around the shoulder joint. One subject had diabetes and three had thyroid disease. The duration of symptoms was defined as the time interval from the onset of pain to the MRI examination. The clinical stage of the adhesive capsulitis was determined based on a system created by Hannafin and Chiaia (14): stage 1 reflected 0-3 months of symptom duration; stage 2, 3-9 months duration; stage 3, 9-15 months duration; and stage 4, 15-24 months duration. Patients with symptoms for longer than 24 months were categorized as stage 4.

### MRI Acquisition

Magnetic resonance imagings were performed using a 3.0T scanner (Magnetom Skyra, Siemens Healthcare, Erlangen, Germany) with a 16-channel shoulder coil from the same vendor (Siemens Healthcare). The scanning parameters for the routine shoulder MRI are summarized in Table 1.

Multi-echo three-dimensional Dixon controlled aliasing in parallel imaging results in higher acceleration (CAIPIRINHA). Volume-interpolated breath-hold examination (VIBE) with T2\*-correction images were acquired in the oblique sagittal plane. The scanning parameters were as follows: matrix = 128 x 101; field-of-view = 300 x 300 mm; repetition time = 9.15 ms; six echoes with echo time = 1.09, 2.46, 3.69, 4.92, 6.15, and 7.38 ms; flip angle = 4°; voxel size = 2.3 x 2.3 x 4.0 mm; slice thickness = 4 mm; number of slices = 40; bandwidth = 1030 Hz/pixel; and acceleration factor = 2. Total acquisition time was 80 seconds. The post-processing algorithm automatically generated fat percentage maps, water percentage maps and effective R2\* maps from the scanner based on a multi-step adaptive fitting method (15)

**Table 1. MRI Parameters for Routine Shoulder Protocol**

	Axial PD TSE FS	Oblique-Sagittal PD TSE	Oblique Coronal PD TSE	Oblique Coronal T2 TSE FS	3D- SPACE PD FS	Multi-Echo Dixon
TR (ms)	4120.0	3770.0	3770.0	4980.0	1000	9.15
TE (ms)	54.0	54.0	54.0	81.0	40.0	1.09, 2.46, 3.69, 4.92, 6.15, 7.38
FOV (mm)	160 x 160	160 x 160	160 x 160	160 x 160	160 x 160	300 x 300
Matrix size	512 x 333	512 x 410	448 x 314	512 x 307	256 x 256	128 x 101
Slice thickness (mm)	3	3	3	3	0.6	4
Slice gap (mm)	0.3	0.6	0.15	0.15		
Voxel size (mm)	0.3 x 0.3	0.3 x 0.3	0.3 x 0.3	0.3 x 0.3	0.6 x 0.6 x 0.6	2.3 x 2.3 x 4.0
Flip angle (°)	136	136	136	136	PD var	4
Averages	1	1	1	2	1	2
ETL	9	9	9	16	71	N/A
Bandwidth (Hz/pixel)	250	250	250	250	349	1030
Slices	26	26	26	26	128	40
Fat suppression	FS			FS	SPAIR	

ETL = echo trains length, FOV = field of view, FS = fat-suppressed, N/A = not available, PD = proton density, PD var = proton density variant (variable flip angles across echo train, suited to PD measurement), SPACE = sampling perfection with application optimized contrasts using different flip-angle evolution, SPAIR = spectral attenuated inversion recovery, TE = echo time, TR = relaxation time, TSE = turbo spin echo

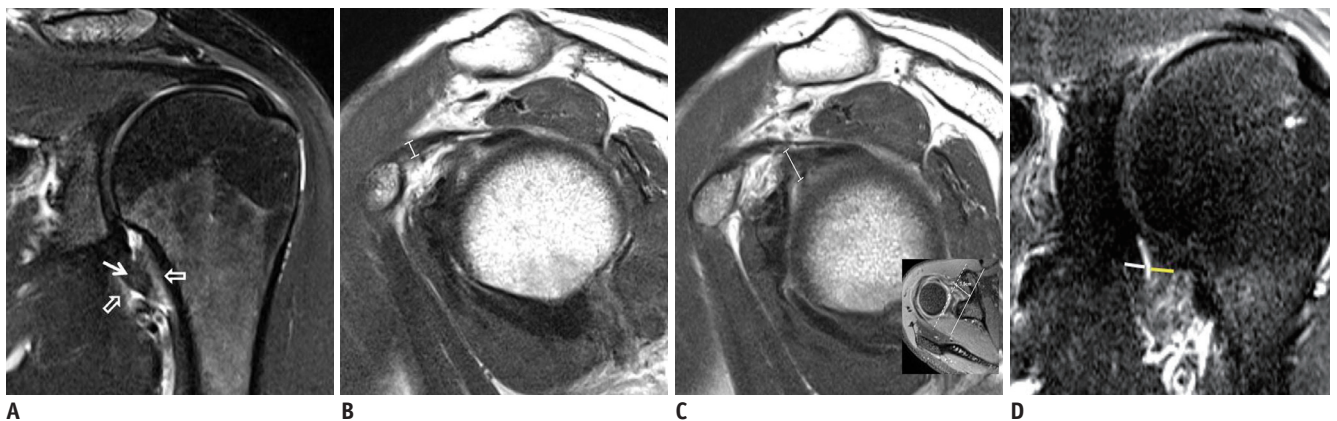


**Fig. 1. 46-year-old woman with clinical diagnosis of adhesive capsulitis.**

**A.** Presence of axillary recess capsular hyperintensity (solid arrow) and extracapsular hyperintensity (open arrows) was evaluated by coronal T2-weighted fat-suppressed imaging. **B.** Thickest portion of coracohumeral ligament (white line) was evaluated on oblique sagittal proton-density-weighted turbo spin-echo images. **C.** Thickest portion of abnormal soft tissue within rotator interval (white line) was measured at 1.5 cm lateral to base of coracoid process on oblique sagittal proton-density-weighted turbo spin-echo images. **D.** Thickness of axillary recess capsules on glenoidal (white line) and humeral (yellow line) sides were measured on oblique coronal images.

using a multiple-peak fat model. Maps were transferred to the picture archiving and communication system (PACS) in 16 bit greyscale using the Digital Imaging and Communications in Medicine format for quantification.

### MRI Interpretation

Magnetic resonance imaging interpretation was performed using our institution's PACS workstation (G3; Infinitt, Seoul, Korea).

Two musculoskeletal radiologists (with 20 and 9 years of experience in radiology, respectively) independently

performed qualitative and quantitative analyses on the conventional MR images. For qualitative analyses, the presence or absence of the following findings was evaluated (Fig. 1A): 1) axillary recess capsular hyperintensity on the oblique coronal T2-weighted fat-suppressed (FS) images (6); and 2) axillary recess extracapsular hyperintensity, defined as high signal intensity outside of the axillary recess capsule on the oblique coronal T2-weighted FS images (6). Subtle findings were categorized as absent. For quantitative analyses, the measurements of adhesive capsulitis MRI findings were calculated based on the methods described

by Mengiardi et al. (5). The thicknesses was calculated by measuring the following parameters: 1) the thickest portion of the CHL on the oblique sagittal images (Fig. 1B); 2) the thickest portion of the abnormal soft tissue in the rotator interval at 1.5 cm lateral to the base of the coracoid process on the oblique sagittal images (Fig. 1C) (representative of thickened capsule, fibrovascular scar tissue and/or synovial hypertrophy); and 3) the thickest portion of the glenoidal and humeral portions of the axillary recess capsule on the oblique coronal images (Fig. 1D). Since the inter-rater agreement was variable and reader 1 had more experience with interpreting musculoskeletal MRIs, reader 1's results of the qualitative and quantitative analyses were used for statistical analyses.

### Fat Quantification

Two radiologists (with 9 and 2 years of experience in radiology, respectively) independently performed fat percentage measurements using the oblique sagittal fat percentage maps of the following shoulder muscles: supraspinatus, infraspinatus, teres minor, subscapularis, teres major, and posterior deltoid. Measurements were made at three locations: at the level of glenoid cartilage and at 1.5 cm and 3 cm medial to the glenoid cartilage (Fig. 2). Regions-of-interest (ROIs) were drawn within 2–3 mm of the muscle boundaries in order to exclude the fat regions at the muscle periphery as described in a previous study (10), and to avoid blurred margins. The mean values obtained from the three locations from both readers were used for statistical analyses.

### Statistical Analysis

All statistical analyses were performed using the SPSS software package, version 16.0 (SPSS Inc., Chicago, IL, USA) and SAS software, version 9.3 (SAS Institute, Cary, NC,

USA). Inter-rater agreement on the quantitative analyses was assessed with intraclass correlation coefficients (ICC). A Cohen kappa analysis was used to evaluate inter-rater reliability for qualitative analyses. The degree of agreement was interpreted as follows: 0.00–0.20 (slight), 0.21–0.40 (fair), 0.41–0.60 (moderate), 0.61–0.80 (substantial) and 0.81–0.99 (almost perfect).

Differences in the fat percentages of the shoulder muscles were assessed using Mann-Whitney U tests for qualitative variables (i.e., the presence or absence of capsular and extracapsular hyperintensities).

Correlations between the mean fat percentages of the shoulder muscles and the quantitative measurements (i.e., the thicknesses of the CHL, abnormal rotator interval soft tissue, and glenoidal/humeral axillary recess capsules), as well as the clinical stages of adhesive capsulitis based on symptom duration were assessed using Spearman's correlation analyses. For the parameters that show statistically significant relationships, partial correlation analyses were performed and controlled for the effects of age, sex and clinical stage. Results were categorized as very strong ( $0.80 < r < 1.0$ ), strong ( $0.60 < r < 0.79$ ), moderate ( $0.40 < r < 0.59$ ), weak ( $0.20 < r < 0.39$ ), or very weak ( $0.00 < r < 0.19$ ).

*P* values of less than 0.05 were considered to represent statistically significant differences.

## RESULTS

The kappa values for the conventional MRI qualitative analyses revealed almost perfect inter-rater reliability (presence or absence of axillary recess capsular hyperintensity,  $k = 0.824$ ; extracapsular hyperintensity,  $k = 0.824$ ). The inter-rater reliabilities for quantitative conventional MRI analyses were as follows: thickness of

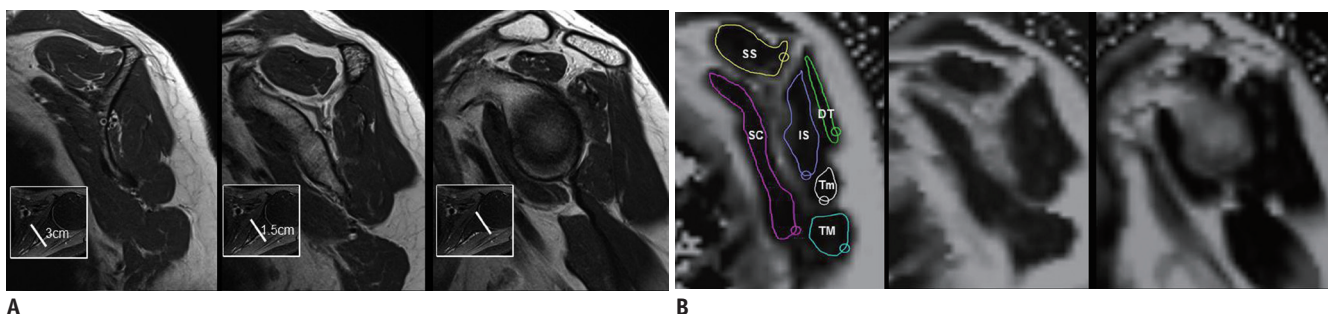


**Fig. 2.** Oblique sagittal proton-density-weighted turbo spin-echo images (A) with respective locations on axial images (small boxes in lower left corner) and corresponding fat percentage maps (B) with region-of-interest placement for fat quantification. Measurements were made at 3 cm and 1.5 cm medial to glenoid cartilage and at level of glenoid cartilage. Note heterogeneous fat distribution in shoulder musculature. DT = deltoid, IS = infraspinatus, SC = subscapularis, SS = supraspinatus, Tm = teres minor, TM = teres major

## Adhesive Capsulitis and Shoulder Muscle Fat Quantification

the CHL (ICC = 0.506); thickness of axillary recess capsule, glenoidal side (ICC = 0.606) and humeral side (ICC = 0.532); and thickness of the abnormal rotator interval soft tissue (ICC = 0.170). Because the inter-rater reliabilities for the quantitative analyses were variable, MRI interpretations made by reader 1, who possessed more experience in interpreting musculoskeletal MRI, were used for statistical analyses.

Inter-observer agreement was almost perfect for fat quantification in all shoulder muscles (supraspinatus, ICC = 0.972; infraspinatus, ICC = 0.978; subscapularis, ICC = 0.992; teres minor, ICC = 0.984; teres major, ICC = 0.985; posterior deltoid, ICC = 0.955); therefore, the mean of both readers were utilized in statistical analyses.

The mean symptom duration was 13 months (range, 1.5–60 months). The total number of patients that were categorized by clinical stage is as follows: stage 1 (n = 7),

stage 2 (n = 7), stage 3 (n = 5), and stage 4 (n = 5).

The mean fat percentages of each shoulder muscle are summarized in Table 2.

For the qualitative analysis, the following MRI findings of adhesive capsulitis were noted by reader 1 included axillary recess capsular hyperintensity (n = 14, 58.3%) and extracapsular hyperintensity (n = 14, 58.3%). For quantitative analysis, the mean thickness of the CHL was  $4.94 \pm 1.45$  mm, and of the abnormal rotator interval soft tissue was  $6.00 \pm 1.27$  mm thick. The capsular thicknesses within the axillary pouch were  $5.26 \pm 1.90$  mm (humeral side) and  $4.80 \pm 1.11$  mm (glenoidal side).

Among the various MRI findings of adhesive capsulitis identified, the Mann-Whitney U test showed a significant difference in the supraspinatus muscle fat percentage in patients with and without extracapsular hyperintensity ( $3.00 \pm 1.74\%$  and  $1.81 \pm 0.80\%$ , respectively,  $p = 0.022$ ).

**Table 2. Mean Fat Percentages of Shoulder Musculature for Each Clinical Stage**

	Clinical Stage	Mean	Standard Deviation	Range
Supraspinatus	Total	2.50	1.53	0.57–8.19
	1	2.65	1.04	1.21–4.46
	2	3.01	2.50	0.57–8.19
	3	2.61	0.62	1.68–3.42
	4	1.15	0.39	0.88–1.80
Infraspinatus	Total	4.23	2.45	1.19–11.62
	1	4.01	1.21	2.11–5.32
	2	4.73	3.35	2.11–11.62
	3	4.67	2.68	2.02–9.06
	4	3.41	2.60	1.19–7.78
Teres minor	Total	3.41	3.12	1.40–13.20
	1	2.13	1.06	1.40–4.40
	2	2.82	1.47	1.64–5.64
	3	4.88	4.70	1.80–13.20
	4	4.55	4.60	1.46–12.46
Subscapularis	Total	3.49	2.86	1.33–15.43
	1	2.80	0.97	1.81–4.66
	2	4.80	4.84	1.57–15.43
	3	3.99	1.93	2.23–6.96
	4	2.13	0.47	1.33–2.50
Teres major	Total	4.49	3.14	1.56–14.53
	1	3.83	2.05	1.56–7.40
	2	5.92	4.99	1.58–14.53
	3	4.99	2.20	2.54–7.37
	4	2.91	0.70	2.20–3.81
Posterior deltoid	Total	2.91	1.85	1.16–10.00
	1	2.38	0.83	1.36–3.70
	2	3.97	2.89	1.92–10.00
	3	2.89	1.60	1.16–5.51
	4	2.16	0.67	1.43–3.13

Moreover, regarding the presence or absence of capsular hyperintensity, there was a clear trend towards different fat percentages in both the subscapularis ( $4.30 \pm 3.52\%$  and  $2.36 \pm 0.75\%$ , respectively,  $p = 0.064$ ) and the teres major ( $5.46 \pm 3.63\%$  and  $3.13 \pm 1.65\%$ , respectively,  $p = 0.064$ ) muscles.

Spearman's correlation showed moderate positive correlation between the teres minor fat percentage and the thickness of the rotator interval abnormal soft tissue ( $r = 0.494$ ,  $p = 0.014$ ) as well as the glenoidal axillary recess capsule ( $r = 0.475$ ,  $p = 0.019$ ). After controlling for the effects of age, sex and clinical stage, a partial correlation analyses showed significant relationships only between the teres minor fat percentage and the thickness of the rotator interval abnormal soft tissue (partial correlation coefficients: rotator interval abnormal soft tissue [ $r = 0.384$ ,  $p = 0.048$ ]; glenoidal axillary recess capsule [ $r = 0.311$ ,  $p = 0.059$ ]).

There were no significant associations between the other adhesive capsulitis MRI findings, clinical stages or other muscular fat percentages ( $p > 0.05$ ). The results of the Mann-Whitney U test and Spearman's correlation analysis are summarized in Table 3.

## DISCUSSION

The etiologies of muscle fatty infiltration can be multifactorial and include muscle disuse and denervation. It has been shown that muscle disuse leads to shortening, increased pennation angle of the muscle fibers, and the filling of spaces created by architectural changes with interstitial fat and fibrosis (16). This study demonstrated that several adhesive capsulitis MRI findings were associated with higher fatty infiltration in shoulder muscles.

In the present study, patients with axillary recess extracapsular hyperintensity tended to have significantly higher fatty infiltration of the supraspinatus muscle. Hyperintensity of the extracapsular portion within the axillary recess is a highly specific MRI finding of adhesive capsulitis with a specificity of 91.2–97% (6), which is a feature that reflects the inflammatory nature of adhesive capsulitis. Recently, Park et al. (17) reported a significant negative correlation between the extracapsular hyperintensity in the axillary recess and the range of motion on abduction ( $B = -23.695$ ,  $p = 0.002$ ) (17). The supraspinatus is a dominant initial abductor of the shoulder (18), and a higher fat percentage in this muscle

**Table 3. Summary of Correlations between MRI Findings, Clinical Stages of Adhesive Capsulitis and Muscle Fat Percentages**

		Axillary Recess Extracapsular Hyperintensity*	Axillary Recess Capsular Hyperintensity*	Thickness of CHL†	Thickness of Abnormal Soft Tissues in Rotator Interval‡	Thickness of Recess Capsule- Glenoidal‡	Thickness of Axillary Recess Capsule-Humeral‡	Clinical Stages of Adhesive Capsulitis‡
Supraspinatus	<i>p</i> value	0.022‡	0.138	0.114	0.722	0.553	0.395	0.083
	Coefficient ( <i>r</i> )			0.331	-0.077	0.127	0.182	0.361
Infraspinatus	<i>p</i> value	1.000	0.666	0.697	0.963	0.886	0.639	0.289
	Coefficient ( <i>r</i> )			-0.084	0.010	0.031	-0.101	-0.226
Teres minor	<i>p</i> value	0.666	0.312	0.329	0.014 (0.048)‡	0.019† (0.059)	0.496	0.126
	Coefficient ( <i>r</i> )			0.208	0.494 (0.384)‡	0.475† (0.311)	0.146	0.321
Subscapularis	<i>p</i> value	0.122	0.064	0.549	0.816	0.788	0.774	0.572
	Coefficient ( <i>r</i> )			0.129	0.050	-0.058	0.062	-0.121
Teres major	<i>p</i> value	0.064	0.064	0.801	0.886	0.883	0.501	0.851
	Coefficient ( <i>r</i> )			-0.054	-0.031	0.032	0.144	-0.040
Posterior deltoid	<i>p</i> value	0.625	0.709	0.809	0.245	0.818	0.530	0.904
	Coefficient ( <i>r</i> )			-0.052	0.247	0.050	-0.135	-0.026

Values in parentheses indicate results from partial correlation analyses with control for age, sex, and clinical stage. \*Two-tailed *p* values from Mann-Whitney U test, †Two-tailed *p* values from Spearman's correlation analysis, ‡Statistically significant differences ( $p < 0.05$ ). *r* = Spearman's correlation coefficient

is correlated with abduction deficit ( $r = 0.45, p < 0.01$ ) (19). Taking all of the above results into consideration, we postulate that axillary recess extracapsular hyperintensity indicated on a MRI scan may be associated with supraspinatus disuse that is possibly due to the decreased range of motion on abduction and results in greater fatty infiltration of the muscle.

In addition, we observed significant associations between the fat infiltration of the teres minor and the thickness of the glenoidal aspect of the axillary recess capsule. A significant negative correlation between the external rotation and axillary joint capsule thickness was demonstrated in a prior study ( $R^2 = 0.34, p = 0.008$ ) (20). The teres minor is an external rotator of the shoulder and fatty infiltration of this muscle is related to a functional external rotation deficit (21). Taking this into account, we propose that a thickened axillary recess capsule indicated on a MRI, especially on the glenoidal side, may be associated with limited external rotation in adhesive capsulitis which would lead to decreased use of the external rotators and eventually further fatty infiltration of the teres minor muscle. However, after adjustment for age, sex and clinical stage, this association was weakened ( $r = 0.475$  to  $0.311$ ) with a considerable trend toward significance ( $p = 0.059$ ).

Previous studies have identified the presence of abnormal soft tissue in the rotator interval as a highly specific finding of adhesive capsulitis (5, 7). We observed various degrees of this finding in all subjects (mean, 6.00 mm; range, 3.87–8.26 mm) and found a positive correlation between the thickness of the abnormal rotator interval soft tissue and the degree of teres minor fatty infiltration. After controlling for the effects of age, sex and clinical stage, this positive association was attenuated ( $r = 0.494$  to  $0.384$ ) but was still statistically significant ( $p = 0.048$ ). It has been suggested that rotator interval abnormalities may be related to inflammation in the early stages of adhesive capsulitis (17); however, our results imply an association between the rotator interval abnormalities and the cumulative chronic changes in the teres minor muscle. It should be noted, though, that the inter-rater reliability for the measurement of the abnormal rotator interval soft tissue was low (ICC = 0.170). Most of the preceding research on the abnormal rotator interval soft tissue in adhesive capsulitis have assessed only for the presence or absence of abnormal soft tissue (17, 20) or obtained measurements using only one reader (5, 20, 22). Furthermore, both readers in the present

study experienced difficulties in the measurement of this abnormal soft tissue, as it was often irregularly shaped, which made consistent measurement more challenging. Therefore, in this study, values measured by a radiologist with more experience in musculoskeletal MRI were used for statistical analysis.

In this study, we performed fat quantification using a multi-echo Dixon method, which has clear advantages over MR spectroscopy in tissues with an uneven fat distribution and spatial heterogeneity like skeletal muscles. Unlike previous studies which used only one image to evaluate fatty infiltration (i.e., the most lateral oblique sagittal image in which the scapular spine is continuous with the body of the scapula (23-25)), we quantified the fat percentages of various shoulder muscles at three different locations. The multi-echo Dixon method allowed for the acquisition of images covering large volumes of the muscles of interest. Additionally, the placement of the ROI was more flexible after image acquisition and could be configured to any size and in multiple sites, which implies less spatial bias than MR spectroscopy (11, 26). Moreover, we were able to assess not only the rotator cuff muscles but also other functionally significant muscles of the shoulder.

Despite its wide use, the Goutallier semi-quantitative grading system has shown a range of inter- and intra-observer reliabilities with few studies yielding unacceptable reliability metrics using this grading system (27-29). However, in agreement with prior studies demonstrating excellent inter-rater reliability of chemical shift-based water-fat imaging in the quantification of muscular fatty infiltration (11, 19), we observed almost perfect inter-rater agreement in the quantification of fat within shoulder muscles using the multi-echo Dixon method. In addition, the feasibility of quantifying early fatty infiltration has been confirmed using a multi-echo Dixon method (11), making it a favorable method in the stratification of patients with early fat infiltration, as in our subjects who had grade 0 or 1 fat infiltration according to the Goutallier grading system.

Regarding the acquisition parameters, we employed a T2\* correction with a multi-echo Dixon method, which demonstrated higher accuracy in the assessment of skeletal muscle fat fractions than two- or three-echo Dixon methods or non-T2\*-corrected Dixon methods (30). In order to compensate for the T1 confounding effects, a low flip angle of 4° was used. We also adopted a multiple-peak fat model for a more robust lipid estimation.

We recognize several limitations in our study. First, the measurement of fat percentages via the multi-echo Dixon method was not validated using MR spectroscopy. However, good correlation between multi-echo Dixon fat quantification and MR muscle spectroscopy has been demonstrated by prior studies (11, 31). Second, the shoulder muscle fat percentages were evaluated only on three oblique sagittal images; more comprehensive evaluations may be needed. Third, a relatively small number of subjects (n = 24) was enrolled in the present study, and we did not evaluate for associations with clinical features, such as pain score and range of motion. Fourth, we included patients with tendinopathy or Ellman classification grade 1 partial rotator cuff tears visible on MRI scans because of the high prevalence of asymptomatic rotator cuff tears (32-34) and our clinical suspicion of adhesive capsulitis that could not be fully explained by a tendinopathy or low-grade partial cuff tears alone. Finally, we could not control for potential confounding variables (i.e., age, sex and clinical stages) in the Mann-Whitney U test. Therefore, additional prospective, age- and gender-matched, case-control studies are needed to adjust for confounding factors.

In conclusion, this study demonstrated associations between several adhesive capsulitis MRI findings and higher fat percentages in the shoulder musculature. In particular, a higher fat percentage in the supraspinatus muscle was seen in patients with extracapsular hyperintensity in the axillary recess. Furthermore, there was a positive correlation between the teres minor fat percentage and the thickness of the abnormal rotator interval soft tissue, after controlling for age, sex and clinical stage. Further studies that determine whether these MRI findings are related to functional and clinical outcome differences may be needed to confirm the potential clinical utility of these MRI findings.

## REFERENCES

- Huang SW, Lin JW, Wang WT, Wu CW, Liou TH, Lin HW. Hyperthyroidism is a risk factor for developing adhesive capsulitis of the shoulder: a nationwide longitudinal population-based study. *Sci Rep* 2014;4:4183
- Neviasser JS. Adhesive capsulitis and the stiff and painful shoulder. *Orthop Clin North Am* 1980;11:327-331
- Neviasser AS, Hannafin JA. Adhesive capsulitis: a review of current treatment. *Am J Sports Med* 2010;38:2346-2356
- Emig EW, Schweitzer ME, Karasick D, Lubowitz J. Adhesive capsulitis of the shoulder: MR diagnosis. *Am J Roentgenol* 1995;164:1457-1459
- Mengiardi B, Pfirrmann CW, Gerber C, Hodler J, Zanetti M. Frozen shoulder: MR arthrographic findings. *Radiology* 2004;233:486-492
- Gondim Teixeira PA, Balaj C, Chanson A, Lecocq S, Louis M, Blum A. Adhesive capsulitis of the shoulder: value of inferior glenohumeral ligament signal changes on T2-weighted fat-saturated images. *Am J Roentgenol* 2012;198:W589-W596
- Connell D, Padmanabhan R, Buchbinder R. Adhesive capsulitis: role of MR imaging in differential diagnosis. *Eur Radiol* 2002;12:2100-2106
- MacDougall JD, Elder GC, Sale DG, Moroz JR, Sutton JR. Effects of strength training and immobilization on human muscle fibres. *Eur J Appl Physiol Occup Physiol* 1980;43:25-34
- Lin HC, Li JS, Lo SF, Shih YF, Lo CY, Chen SY. Isokinetic characteristics of shoulder rotators in patients with adhesive capsulitis. *J Rehabil Med* 2009;41:563-568
- Rawat P, Eapen C, Seema KP. Effect of rotator cuff strengthening as an adjunct to standard care in subjects with adhesive capsulitis: A randomized controlled trial. *J Hand Ther* 2017;30:235-241.e8
- Agten CA, Roskopf AB, Gerber C, Pfirrmann CW. Quantification of early fatty infiltration of the rotator cuff muscles: comparison of multi-echo Dixon with single-voxel MR spectroscopy. *Eur Radiol* 2016;26:3719-3727
- Fischer MA, Nanz D, Shimakawa A, Schirmer T, Guggenberger R, Chhabra A, et al. Quantification of muscle fat in patients with low back pain: comparison of multi-echo MR imaging with single-voxel MR spectroscopy. *Radiology* 2013;266:555-563
- Ellman H. Diagnosis and treatment of incomplete rotator cuff tears. *Clin Orthop Relat Res* 1990;64-74
- Hannafin JA, Chiaia TA. Adhesive capsulitis. A treatment approach. *Clin Orthop Relat Res* 2000:95-109
- Zhong X, Nickel MD, Kannengiesser SA, Dale BM, Kiefer B, Bashir MR. Liver fat quantification using a multi-step adaptive fitting approach with multi-echo GRE imaging. *Magn Reson Med* 2014;72:1353-1365
- Meyer DC, Hoppeler H, von Rechenberg B, Gerber C. A pathomechanical concept explains muscle loss and fatty muscular changes following surgical tendon release. *J Orthop Res* 2004;22:1004-1007
- Park S, Lee DH, Yoon SH, Lee HY, Kwack KS. Evaluation of adhesive capsulitis of the shoulder with fat-suppressed T2-weighted MRI: Association between clinical features and MRI findings. *Am J Roentgenol* 2016;207:135-141
- Ackland DC, Pak P, Richardson M, Pandy MG. Moment arms of the muscles crossing the anatomical shoulder. *J Anat* 2008;213:383-390
- Nardo L, Karampinos DC, Lansdown DA, Carballido-Gamio J, Lee S, Maroldi R, et al. Quantitative assessment of fat infiltration in the rotator cuff muscles using water-fat MRI. *J Magn Reson Imaging* 2014;39:1178-1185
- Ahn KS, Kang CH, Oh YW, Jeong WK. Correlation between magnetic resonance imaging and clinical impairment in patients with adhesive capsulitis. *Skeletal Radiol*

- 2012;41:1301-1308
21. Walch G, Boulahia A, Calderone S, Robinson AH. The 'dropping' and 'hornblower's' signs in evaluation of rotator-cuff tears. *J Bone Joint Surg Br* 1998;80:624-628
  22. Jung JY, Jee WH, Chun HJ, Kim YS, Chung YG, Kim JM. Adhesive capsulitis of the shoulder: evaluation with MR arthrography. *Eur Radiol* 2006;16:791-796
  23. Goutallier D, Postel JM, Bernageau J, Lavau L, Voisin MC. Fatty muscle degeneration in cuff ruptures. Pre- and postoperative evaluation by CT scan. *Clin Orthop Relat Res* 1994;78-83
  24. Fuchs B, Weishaupt D, Zanetti M, Hodler J, Gerber C. Fatty degeneration of the muscles of the rotator cuff: assessment by computed tomography versus magnetic resonance imaging. *J Shoulder Elbow Surg* 1999;8:599-605
  25. Tae SK, Oh JH, Kim SH, Chung SW, Yang JY, Back YW. Evaluation of fatty degeneration of the supraspinatus muscle using a new measuring tool and its correlation between multidetector computed tomography and magnetic resonance imaging. *Am J Sports Med* 2011;39:599-606
  26. Fox PT. Physiological ROI definition by image subtraction. *J Cereb Blood Flow Metab* 1991;11:A79-A82
  27. Oh JH, Kim SH, Choi JA, Kim Y, Oh CH. Reliability of the grading system for fatty degeneration of rotator cuff muscles. *Clin Orthop Relat Res* 2010;468:1558-1564
  28. Slabaugh MA, Friel NA, Karas V, Romeo AA, Verma NN, Cole BJ. Interobserver and intraobserver reliability of the Goutallier classification using magnetic resonance imaging: proposal of a simplified classification system to increase reliability. *Am J Sports Med* 2012;40:1728-1734
  29. Lesage P, Maynou C, Elhage R, Boutry N, Hérent S, Mestdagh H. [Reproducibility of CT scan evaluation of muscular fatty degeneration. Intra- and interobserver analysis of 56 shoulders presenting with a ruptured rotator cuff muscles]. *Rev Chir Orthop Reparatrice Appar Mot* 2002;88:359-364
  30. Yoo YH, Kim HS, Lee YH, Yoon CS, Paek MY, Yoo H, et al. Comparison of multi-echo Dixon methods with volume interpolated breath-hold gradient echo magnetic resonance imaging in fat-signal fraction quantification of paravertebral muscle. *Korean J Radiol* 2015;16:1086-1095
  31. Reeder SB, Robson PM, Yu H, Shimakawa A, Hines CD, McKenzie CA, et al. Quantification of hepatic steatosis with MRI: the effects of accurate fat spectral modeling. *J Magn Reson Imaging* 2009;29:1332-1339
  32. Yamaguchi K, Tetro AM, Blam O, Evanoff BA, Teefey SA, Middleton WD. Natural history of asymptomatic rotator cuff tears: a longitudinal analysis of asymptomatic tears detected sonographically. *J Shoulder Elbow Surg* 2001;10:199-203
  33. Reilly P, Macleod I, Macfarlane R, Windley J, Emery RJ. Dead men and radiologists don't lie: a review of cadaveric and radiological studies of rotator cuff tear prevalence. *Ann R Coll Surg Engl* 2006;88:116-121
  34. Needell SD, Zlatkin MB, Sher JS, Murphy BJ, Uribe JW. MR imaging of the rotator cuff: peritendinous and bone abnormalities in an asymptomatic population. *Am J Roentgenol* 1996;166:863-867